Metabolic Engineering 43 (2017) 21–28

Contents lists available at ScienceDirect

Metabolic Engineering

journal homepage: www.elsevier.com/locate/meteng

Pathway optimization and key enzyme evolution of *N*-acetylneuraminate biosynthesis using an *in vivo* aptazyme-based biosensor

Peng Yang, Jing Wang, Qingxiao Pang, Fengyu Zhang, Junshu Wang, Qian Wang*, Qingsheng Qi*

State Key Laboratory of Microbial Technology, National Glycoengineering Center, Shandong University, Jinan 250100, People's Republic of China

ARTICLE INFO

Keywords:
Biosensor
Genetic selection
N-acetylneuraminate
Pathway optimization
NeuAc synthase

ABSTRACT

N-acetylneuraminate (NeuAc) biosynthesis has drawn much attention owing to its wide applications in many aspects. Previously, we engineered for the first time an artificial NeuAc biosynthetic pathway in *Escherichia coli* using glucose as sole substrate. However, rigorous requirements for the flux and cofactor balance make subsequent strain improvement rather difficult. In this study, an *in vivo* NeuAc biosensor was designed and applied for genetic screening the mutant library of NeuAc producer. Its NeuAc responsive manner was demonstrated using *sfgfp* as a reporter and a Ni^{2+}-based selection system was developed to couple the cell growth with *in vivo* NeuAc concentration. Employing this selection system, the NeuAc biosynthesis pathway was optimized and the key enzyme NeuAc synthase was evolved, which improved the titer by 34% and 23%, respectively. The final strain produced up to 8.31 g/L NeuAc in minimal medium using glucose as sole carbon source. This work demonstrated the effectiveness of NeuAc biosensor in genetic screening and great potential in metabolic engineering of other organisms.

1. Introduction

Thirty years of metabolic engineering practice has resulted in a tremendous increase in microbial manufacturing of value-added compounds, including pharmaceuticals, biofuels, organic acids and polymer precursors among others (Liang and Qi, 2014; Zhang et al., 2016). The most predominant sialic acids-*N*-acetylneuraminate (NeuAc) has been intensively studied these years due to its enormous potential in edible and pharmaceutical applications (Kang et al., 2012; Tao et al., 2010). Compared with enzymatic conversion or whole-cell catalysis methods, direct fermentative NeuAc production from glucose holds certain advantages since it can synthesize NeuAc in one step without adding any direct precursors (Fig. 1). We previously constructed a GlcNAc-6-P-centered NeuAc biosynthetic pathway in *Escherichia coli* by overexpressing a feedback resistant GlcN-6-P synthase (*glmS**), a GlcN-6-P *N*-acetyltransferase (*GNA1*), a GlcNAc 2-epimerase (*slr1975*), and an endogenous NeuAc adolase (*nanA*), which demonstrated the possibility of fermentative production of NeuAc from glucose without adding any precursor (Kang et al., 2012). However, the low yield and productivity of NeuAc was far from the theoretical maximum (0.86 g/g glucose), which indicates large space for further improvement. Nevertheless, attempt *via* rational design progressed slowly due to our limited understanding for the complex physiology of the producer strain.

In this sense, directed evolution which acts top-down on biological functions rather than mechanisms is a more efficient way to achieve biological design goals (Bassalo et al., 2016). This strategy comprises two main steps. Firstly, a mutant library of large diversity shall be created. Then, using appropriate screen/selection methods, desired phenotype was identified and evaluated. Desired mutants can be readily identified if growth-related phenotype is favored (Alper et al., 2006; Warnecke et al., 2008) or the target product is colored (DeLoache et al., 2015; Wang et al., 2009; Watstein et al., 2015). For most target products of interest including NeuAc, however, there is an evaluation bottleneck due to their lack of conspicuous phenotype and therefore requirement for costly and labor-intensive technologies such as gas chromatography, high-performance liquid chromatography, mass spectrometry or NMR (throughput $< 10^3$ samples per machine per day) (Raman et al., 2014). Thus, biosensors that detect a desired metabolite and transduce its presence into a quantifiable signal (selectable/screenable) will boost the evaluation capacity dramatically in metabolic engineering process (Liu et al., 2015; Rogers et al., 2016).

Biosensors comprise a sensor part (*e.g.* riboswitches, ribozymes, transcription factors, enzymes and periplasmic-binding proteins) and an actuator part (*e.g.* fluorescent reporters, regulatory switches or selection markers) (Michener et al., 2012). Upon binding of the effector molecules, a conformational change in the sensor part would in turn control the expression of the actuator part in a ligand-dependent manner. Fortunately, a previously reported NeuAc aptamer with high

* Corresponding authors.
E-mail addresses: qiqi20011983@gmail.com (Q. Wang), qiqingsheng@sdu.edu.cn (Q. Qi).

http://dx.doi.org/10.1016/j.ymben.2017.08.001
Received 3 June 2017; Received in revised form 18 July 2017; Accepted 1 August 2017
Available online 02 August 2017

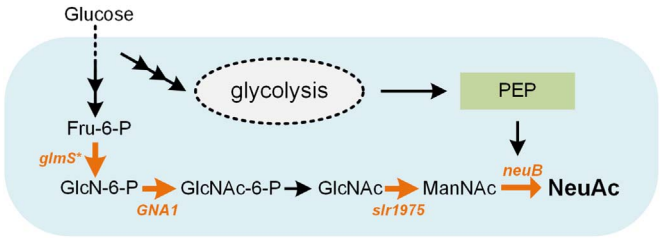

Fig. 1. Schematic presentation of NeuAc synthesis pathway in engineered *E. coli*. Genes: *glmS**, feedback resistant GlcN-6-P synthase; *GNA1*, GlcN-6-P *N*-acetyltransferase; *slr1975*, GlcNAc 2-epimerase; *neuB*, NeuAc synthase. Abbreviations: Fru-6-P, fructose-6-phosphate; PEP, phosphoenolpyruvate; GlcN-6-P, glucosamine-6-phosphate; GlcNAc-6-P, *N*-acetylglucosamine-6-phosphate; GlcNAc, *N*-acetylglucosamine; ManNAc, *N*-acetylmannosamine; NeuAc, *N*-acetylneuraminate.

specificity and affinity (~ 1.35 nM) serves as an excellent candidate for constructing an *in vivo* active NeuAc biosensor (Cho et al., 2013).

With the established *in vitro/in vivo* sensor design methods (Joyce, 2004; Lynch et al., 2007; Muranaka et al., 2009; Tang et al., 2013) and the principles for biosensor construction (Ceres et al., 2013; Win and Smolke, 2007), biosensors can be readily engineered to respond to any new metabolites virtually. Till now, it has been recognized that biosensor-facilitated directed evolution is efficient for dynamically modulating pathway flux (Xu et al., 2014; Zhang et al., 2012), improving the activity, stability and region-selectivity of key enzymes (DeLoache et al., 2015; Michener and Smolke, 2012; Wang et al., 2015), or increasing the titer of specified product (Binder et al., 2012; Raman et al., 2014; Zhou and Zeng, 2015).

In this study, we designed an *in vivo* active biosensor that responds to NeuAc in a dose-dependent fashion for the first time. Under selection condition, intracellular NeuAc concentration was coupled with the cell growth correspondingly. With the biosensor-facilitated high-throughput mutants screening, NeuAc titer increased from 1.58 g/L to 2.61 g/L, demonstrating the effectiveness of this device in metabolic engineering of NeuAc producer. Also, this work should be suggestive for the development and utilization of other aptazyme-based biosensors.

2. Materials and methods

2.1. Bacterial strains, plasmids and media

Bacterial strains and plasmids used in this study are listed in Supplementary Table 1. *E. coli* DH5α and MG1655 were used for cloning purposes and were propagated in Luria-Bertani (LB) medium at 37 °C under aeration. For Ni^{2+}-based selection, M9B minimal medium was used. This medium contained (per liter): 6 g KH_2PO_4, 24 g K_2HPO_4, 1 g $Na_3Citrate{\cdot}2H_2O$, 10 g $(NH_4)_2SO_4$, 0.6 g $MgSO_4{\cdot}7H_2O$ and 0.025 g $CaCl_2{\cdot}2H_2O$. The trace elements were supplied as follows (per liter): 0.01 mg $CoCl_2{\cdot}6H_2O$, 0.01 mg H_3BO_3, 0.01 mg $CoSO_4{\cdot}5H_2O$, 0.5 mg $FeSO_4{\cdot}7H_2O$, 0.033 mg $MnSO_4{\cdot}H_2O$, 0.38 mg $ZnSO_4{\cdot}7H_2O$ and 0.01 mg $NaMoO_4{\cdot}2H_2O$. Modified terrific broth (MTB) medium (12 g/L tryptone, 24 g/L yeast extract and 5 g/L NaCl) was used for NeuAc batch fermentation. Antibiotics were added when necessary (ampicillin 100 μg/mL, kanamycin 25 μg/mL, chloramphenicol 17 μg/mL, tetracycline 10 μg/mL and spectinomycin 100 μg/mL). Vitamin B1 was added to a final concentration of 10 μg/mL when necessary.

2.2. Plasmid construction

Oligonucleotides used in this work are listed in Supplementary Table 2. A high-fidelity DNA polymerase (Takara, Japan) was used for plasmid construction purpose and 2×Taq MasterMix (CWBIO, China) was used for colony PCR. pS-gfp (Supplementary Figure 1) was constructed as follows. s*fgfp* gene with ssrA degrading label was generated by PCR with primers gfp-F and gfp-R, using psfGFP-ssrA as the template. To extend homology arm, resulting fragment was used as template to perform another cycle of PCR using primers S2 and gfp-R, generating fragment *gfp*2. Plasmid pTrc99a digested with *Eco*RI and *Bam*HI was used as the backbone after gel purification. Then, *gfp*2, digested pTrc99a and primer S1 were assembled together using a single strand assembly method (Coussement et al., 2014). Plasmid pS-tetA was constructed by amplifying *tetA* with primers tetA-F and tetA-R using pUC19-tetA as the template and cloning into the *Eco*RI and *Not*I sites of pS-gfp. To construct p-gfp and p-tetA, PCR amplification of pS-gfp and pS-tetA using primers ds-F and ds-R was performed. Resulting fragment was then electrotransformed into *E. coli* MG1655 after *Dpn*I digestion.

Plasmid pB was constructed by amplifying *neuB* (NeuAc synthase, GenBank: AEQ. 14203.1) with primers neuB-F and neuB-R from genomic DNA of *E. coli* K1 and cloning into the *Spe*I and *Not*I sites of pNnsGM. The *tetA*-biosensor was amplified from pS-tetA using primers s-F1 and s-R1. After digestion with *Kpn*I and *Xho*I, the biosensor was cloned into pNnsGM and pB treated with the same restriction endonucleases, generating pSA and pSB. A bidirectional terminator was used to prevent mutual interference.

For p15A-S construction, the *tetA*-biosensor was amplified from pS-tetA using primers s-F2 and s-R2. After digestion with *Eco*RI and *Bam*HI, the biosensor was cloned into pMCL200 treated with the same restriction endonucleases. Plasmid pB-based randomized RBS mutant library was generated as follows. The backbone was amplified from pB using primers pB-F1 and pB-R1. For library 1, the four genes with randomized RBS were amplified from pB using degenerate primers neuB-F1/neuB-R1, slr-F1/slr-R1, GNA1-F1/GNA1-R1 and glmS-F1/glmS-R1, respectively. The degenerate RBSs were designed using RBS Calculator v2.0 without nucleotide constraints. For library 2, the four genes were amplified using degenerate primers neuB-Fc/neuB-Rc, slr-Fc/slr-Rc, GNA1-Fc/GNA1-Rc and glmS-Fc/glmS-R1. Then the five fragments were assembled together using the Gibson method (Gibson et al., 2009). Positive rates of the libraries were determined by performing colony PCR using primers pB-testF/pB-testR.

For p4ks construction, pCL1920 digested with *Sal*I and *Kpn*I was used as the backbone. *NeuB* was amplified from p2e using primers neuB-F2 and neuB-R2. *Slr1975-GNA1-glmS* was amplified from p2e using primers 3-F and 3-R. The *tetA*-biosensor was amplified from pS-tetA using primers s-F3 and s-R3. Then the four fragments were assembled together using the Gibson method. NeuB mutant library was generated as follows. Error-prone PCR was performed using GeneMorph II Random Mutagenesis kit (Agilent Technologies, USA) following the manufacturer's instructions. Randomly mutated *neuB* was amplified from p4ks using primers neuB-F3 and neuB-R2 and then cloned into p4ks digested with *Sal*I and *Kpn*I.

For NeuB purification, expression plasmids were created based on pET28a containing the T7 promoter. Wild type and mutant NeuB were amplified from p4ks or enriched plasmids using primers neuB-F4 and neuB-R4 and then cloned into pET28a digested with *Bam*HI using the Gibson method.

2.3. Strain cultivation

For *gfp*-biosensor characterization, a single colony was inoculated into 5 mL LB and incubated for 12 h at 37 °C and 200 rpm. The preculture was inoculated into 50 mL of fresh LB containing 30 g/L glucose with 2% inoculum. Then different amounts of NeuAc (0 mM, 6 mM, 12 mM) were added to the culture. Cultivation was maintained at 37 °C and 220 rpm. The fluorescence intensity was determined at 6–10 h intervals.

For *tetA*-biosensor characterization, a single colony was inoculated into 5 mL LB and incubated for 12 h at 37 °C and 200 rpm. The preculture was then inoculated into 50 mL of fresh M9B minimal medium containing 20 g/L glucose and 50 μM Ni^{2+} with 1% inoculum. Different amounts of NeuAc (0–100 mM) were added to the culture at start. Cultivation was maintained at 37 °C and 220 rpm. Samples were taken

at 4 h intervals for analysis. To perform genetic selection, M9B minimal medium with 20 g/L glucose, 10 μg/mL vitamin B1, 50 μM Ni^{2+}, 10 μg/mL tetracycline and 200 μM IPTG was used. When cells reached to the late-exponential stage (OD_{600} of 1.0–1.2), the culture was transferred to fresh selection medium with 1% inoculum. After three serial cultivations, representing one enrichment cycle, plasmids were extracted and re-transformed into fresh parental strain to perform the next cycle.

To perform NeuAc batch fermentation, a single colony was inoculated into 5 mL LB medium containing the appropriate antibiotics and incubated for 12 h at 37 °C. The pre-culture was then inoculated into 50 mL of fresh MTB medium containing 30 g/L glucose and 200 μM IPTG with 4% inoculum. Fermentation was performed at 37 °C and 220 rpm, and pH was maintained at approximate 7.0 by 30% NH_4OH throughout the fermentation. Samples were taken at 6 h intervals for analysis. For experiments performed in 24-well plates, 37 °C and 500 rpm was used (using a TAITEC M.BR-022UP bioshaker).

For two-stage fermentation, a single colony was inoculated into 50 mL LB medium and incubated for 12 h at 37 °C. The pre-culture was then inoculated into a second culture (150 mL M9B minimal medium supplemented with 5 g/L yeast extract, 1% glucose and 200 μM IPTG in a 1-L shake flask) with 4% inoculum. The cells were harvested at an OD_{600} of 7–10 by centrifugation (4000 rpm, 4 °C, 10 min) and re-suspended in 50 mL solution buffer (44 mM KH_2PO_4, 137 mM K_2HPO_4 and 75 mM $(NH_4)_2SO_4$) to an appropriate cell density in a 300-mL baffled shake flask. The initial glucose concentration was 30 g/L and glucose was added when its concentration was below 5 g/L. Fermentation was performed at 37 °C and 180 rpm, and pH was maintained at approximate 7.0 by 30% NH_4OH throughout the fermentation. Samples were taken at 4–6 h intervals for analysis.

2.4. Purification of NeuAc synthase and activity assay

Recombinant *E. coli* BL21(DE3) strains expressing wild type or mutant NeuB containing a N-terminal 6His-tag were disrupted by ultrasonication and target enzymes were purified by Ni-NTA Agarose column (Column purchased from Bio-Rad was 1 cm in diameter and packed with the total volume of 1 mL Ni-NTA Agarose beads purchased from Qiagen) (Ji et al., 2015). For enzyme activity assay, samples of enzyme were incubated with 10 mM ManNAc, 8.75 mM PEP in a final volume of 250 μL of 125 mM Tris buffer, pH 7.0, at 37 °C for 15 min and the reaction was stopped by heating at 100 °C for 3 min. Then formation of NeuAc was determined by a resorcinol-based colorimetric assay (Hooks et al., 2013). One unit of enzyme activity (U) was defined as the amount of enzyme catalyzing the formation of 1 μM NeuAc per min at 37 °C. Protein concentrations were determined by the method of Bradford (Bradford, 1976), using bovine serum albumin as a standard.

2.5. Analytical methods

Optical density (OD) was measured at 600 nm with a spectrophotometer (Shimazu, Japan). Fermentation samples were centrifuged at 12,000 rpm for 5 min and the supernatant was used for extracellular metabolites detection. The precipitate was disrupted by ultrasonication for intracellular NeuAc detection. Glucose, NeuAc, acetate, ethanol, formate, pyruvate, GlcNAc and ManNAc were quantitatively determined by HPLC (Shimadzu, Japan) equipped with a refractive index detector (RID-10A) (Shimadzu, Japan) and an Aminex HPX-87H ion exclusion column (Bio-Rad, USA) as described previously (Li et al., 2013). NeuAc levels were additionally determined by a resorcinol-based colorimetric assay (Hooks et al., 2013). Green fluorescence (excitation at 485 nm and emission at 528 nm) was detected using a Multi-Detection Microplate Reader (Synergy HT, Biotek, USA).

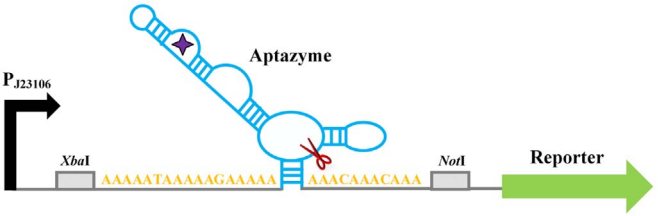

Fig. 2. Design strategy of the NeuAc biosensor. The bent arrow in black indicates the constitutive promoter P_{J23106} (http://parts.igem.org/Main_Page). Binding of the ligand (star in purple) would induce a self-cleavage of the aptazyme (in blue) and destabilize the mRNA of downstream reporter gene (in green). A 'buffer sequence' (in orange) was used to insulate the aptazyme from surrounding sequences. (For interpretation of the references to color in this figure legend, the reader is referred to the web version of this article).

3. Results and discussion

3.1. Design of an in vivo active NeuAc biosensor

To couple the intracellular NeuAc concentration with a conspicuous readout, we designed an aptazyme-based biosensor (Fig. 2). The designed NeuAc biosensor is analogous to the naturally occurred ligand-responsive ribozyme (*e.g.* the *glmS* ribozyme) (Winkler et al., 2004). Upon binding of its ligand (NeuAc in this study), a conformational change in the sensor part would lead to the self-cleavage of the ribozyme, thus destabilize the mRNA of downstream gene (*gfp* or *tetA* in this study) and decrease its expression. Through fusion of the core binding region of a previously selected NeuAc aptamer to the stem II of hammerhead ribozyme (Cho et al., 2013), a NeuAc-specific aptazyme was engineered. Then, we fused the aptazyme with the sfGFP fluorescence reporter through a 'buffer sequence' to insulate the aptazyme from surrounding sequences, yielding plasmid pS-gfp. A similar construct lacking the aptazyme (p-gfp) was used as the negative control.

To characterize the designed NeuAc sensor *in vivo*, exogenous NeuAc ranging from 0 mM to 12 mM was added to DH5α strains harboring plasmid pS-gfp or p-gfp, and the resulting fluorescence intensity was measured 24 h and 48 h after NeuAc addition. As shown in Fig. 3A, the fluorescence intensity decreased at both 24 h and 48 h in DH5α/pS-gfp with increased exogenous NeuAc addition, while no obvious fluorescence alteration was observed in negative control. With 12 mM NeuAc added, there was about a 6.2-fold inhibition of the fluorescence at 24 h and 11.8-fold at 48 h.

In a previous study, 1 mM 2-aminopurine or theophylline was used to activate biosensors in *E. coli* (Ceres et al., 2013). Considering the decomposition of NeuAc by the *nanATEK* operon in DH5α, 6 mM or 12 mM NeuAc concentration was arbitrarily adopted. Also note that when 0 mM NeuAc was added, the fluorescence intensity of DH5α/pS-gfp was comparable to that of DH5α/p-gfp, which suggests that insertion of the NeuAc aptazyme at the 5′ UTR did not interfere with downstream reporter gene transcription or translation significantly. This result demonstrated that an *in vivo* active NeuAc biosensor was successfully constructed.

Then, reporter gene *tetA* was fused to the NeuAc aptazyme (generating pS-tetA) to develop a Ni^{2+}-based selection system for growth-coupled selection. *TetA* encodes a tetracycline/H^+ antiporter and can be used as both a positive and a negative selection marker. TetA confers the cells tetracycline resistance while renders them more sensitive to toxic metal salts such as $NiCl_2$ (Muranaka et al., 2009). The NeuAc biosensor would enable cells that accumulate more intracellular NeuAc to survive in the presence of $NiCl_2$. To minimize interference, a modified M9 minimal medium previously used to produce *N*-acetylglucosamine was adopted (Deng et al., 2005). In a preliminary experiment, we determined the optimal selection concentration of Ni^{2+} in this medium to be 50 μM, because under this concentration, growth inhibition caused by *tetA* expression was more obvious (Supplementary

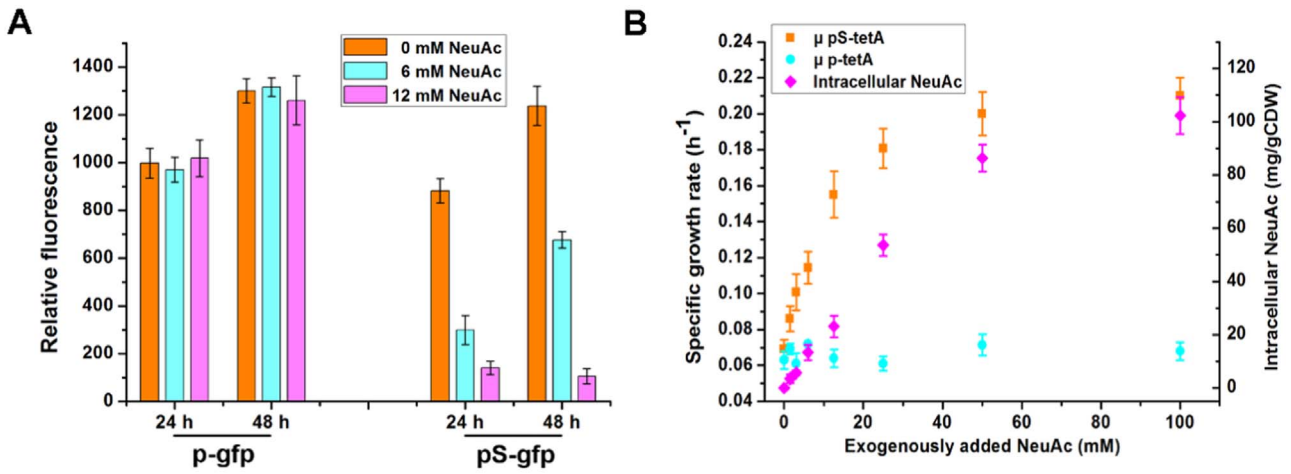

Fig. 3. *In vivo* characterization of the NeuAc biosensor. (A) Using *sfgfp* as the reporter gene, effects of exogenously added NeuAc on the fluorescence intensity of DH5α/p-gfp or DH5α/pS-gfp were shown. Strains were cultured in LB medium with 3% glucose. The fluorescence intensity of sfGFP was normalized by OD_{600}. (B) Using *tetA* as the reporter gene, effects of exogenously added NeuAc on intracellular NeuAc and cell growth of DH5α/p-tetA or DH5α/pS-tetA were shown. Strains were cultured in M9B minimal medium with 3% glucose and 50 μM Ni^{2+}. Results are averages from three independent experiments, with standard deviations indicated by error bars.

Figure 2). A similar construct lacking the aptazyme (p-tetA) was used as the negative control.

Then specific growth rate on response of exogenously added NeuAc was determined. As we can see in Fig. 3B, with increased level of exogenous NeuAc (from 0 to 100 mM), cell grew better under selection conditions. In contrast, cell growth was relatively poor regardless of exogenous NeuAc in the control. We also quantitatively determined the intracellular NeuAc concentration. As exogenous NeuAc addition increased, the intracellular NeuAc concentration rose correspondingly. On a concentration range of 0–86.4 ± 5.1 mg/gCDW intracellular NeuAc (0–50 mM exogenous NeuAc addition), the biosensor works soundly. Above this concentration, cell growth advantage under Ni^{2+} selection becomes not obvious. Taken these together, our designed biosensor has a large operational range and can be used for selection of high NeuAc producer. Operational range of a sensor is very important. When small amount of target product accumulated, a sensor with high affinity was beneficial. If substantial accumulation of target product occurred, a sensor with low affinity would be helpful. In addition to aptamer modification, operational range of sensors can also be tuned by promoter swapping, change of sensor copies or activating an exporter of target product.

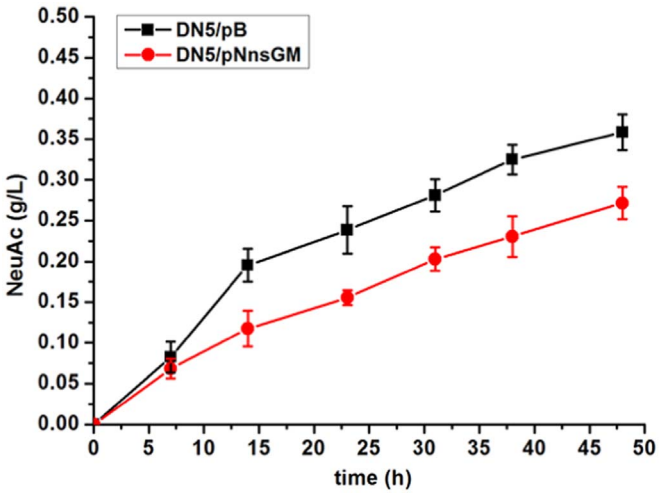

Fig. 4. Fermentation of DN5/pB and DN5/pNnsGM. Strains were cultivated in M9B minimal medium at 37 °C and 250 rpm with 20 g/L glucose, and pH was maintained at approximate 7.0. Results are averages from three independent experiments, with standard deviations indicated by error bars.

3.2. Validation of the selection system using model library

To demonstrate the feasibility of the NeuAc biosensor for genetic selection, an enrichment assay using defined model libraries was performed as a proof of concept. Plasmid pNnsGM harboring *nanA*, *slr1975*, *GNA1* and mutant *glmS* gene was previously constructed for NeuAc production (Kang et al., 2012). NanA catalyzes the reversible aldol condensation of NeuAc from ManNAc and pyruvate. However, equilibrium of the reaction favors NeuAc cleavage rather than synthesis, which leads to low yield and efficiency for NeuAc production (Uchida et al., 1984). To increase NeuAc yield from glucose, an irreversible NeuAc synthase NeuB was employed instead of NanA, generating plasmid pB. We compared the NeuAc production capacity of DN5/pB with DN5/pNnsGM in M9B minimal medium. As a result, DN5/pB produced 0.36 ± 0.02 g/L NeuAc in 48 h while DN5/pNnsGM produced 0.27 ± 0.02 g/L NeuAc (Fig. 4). Also as expected, the intracellular NeuAc concentration of DN5/pB (67.6 ± 4.7 mg/gCDW) was higher than that of DN5/pNnsGM (49.2 ± 2.8 mg/gCDW).

The *tetA*-NeuAc biosensor was then cloned into pB and pNnsGM, generating pSB and pSA, respectively. A mixture of two species DN5/pSB and DN5/pSA at 1:100 ratio was cultured in M9B medium with/without 50 μM Ni^{2+}. Tetracycline was added to a final concentration of 10 μg/mL to prevent accumulation of inactive TetA mutants. When cells reached to the late-exponential stage, the culture was transferred to fresh selection medium. After three serial cultivations, representing one enrichment cycle, the culture was subjected to single colony isolation. Colony PCR was performed to evaluate the proportion of pSB and pSA.

For a total of 3 independent replicates of the experimental group, the proportion of pSB was 4/24, 6/24 and 6/24 respectively. This meant a more than 16-fold enrichment of the high NeuAc producer DN5/pSB. On the contrary, the proportion of pSB was 0/24, 1/24 and 0/24 for the control group (Supplementary Figure 3). Previously, biosensors were used to enrich target mutant from a pool of 10^4–10^6 excess background cells (Desai and Gallivan, 2004; Muranaka et al., 2009). Here, a 1:100 dilution rate was chosen to ensure an easily detectable enrichment ratio within one single selection cycle. This result further demonstrated the feasibility of the designed NeuAc-biosensor in facilitating selection process during microbial evolution or pathway optimization.

Table 1
Distinction of the designed degenerate RBSs between library1 and 2.

	Gene	Degenerate RBS[a]	Library size	Translation initiation rate (au)[b]
Library 1	*neuB*	TTA**MDM**G**M**CGTATACAAAAAAATACGGAGGTCCAT	24	1417.9–29312.2
	slr1975	AGAAA**B**AG**M**AATATATT**B**TTC**K**AGAGGAGGTACA	36	1361.7–45562.3
	GNA1	TAGTAATATTCT**M**C**K**TTCGTC**V**AGGAGGT**Y**ATCTG	24	2171.5–21947.6
	glmS	TT**M**TTTCAAA**K**CAT**H**TTAATATAAGTAGGTATA**W**A	24	1973.9–20496.4
Library 2	*neuB*	TAACTACATAAAT**M**AGG**MR**G**W**ATCAC	16	434.1–73580.4
	slr1975	TAACTACATAAAT**M**AGG**MR**G**W**ATCAC	16	128.8–36793.1
	GNA1	TAACTACATAAAT**M**AGG**MR**G**W**ATCAC	16	202.2–12705.5
	glmS	TAACTACATAAAT**M**AGG**MR**G**W**ATCAC	16	531.5–72267.7

[a] Degenerate bases were shown in bold and underlined.
[b] Translation initiation rates of the RBSs were predicted with the RBS Calculator v2.0 (Salis et al., 2009).

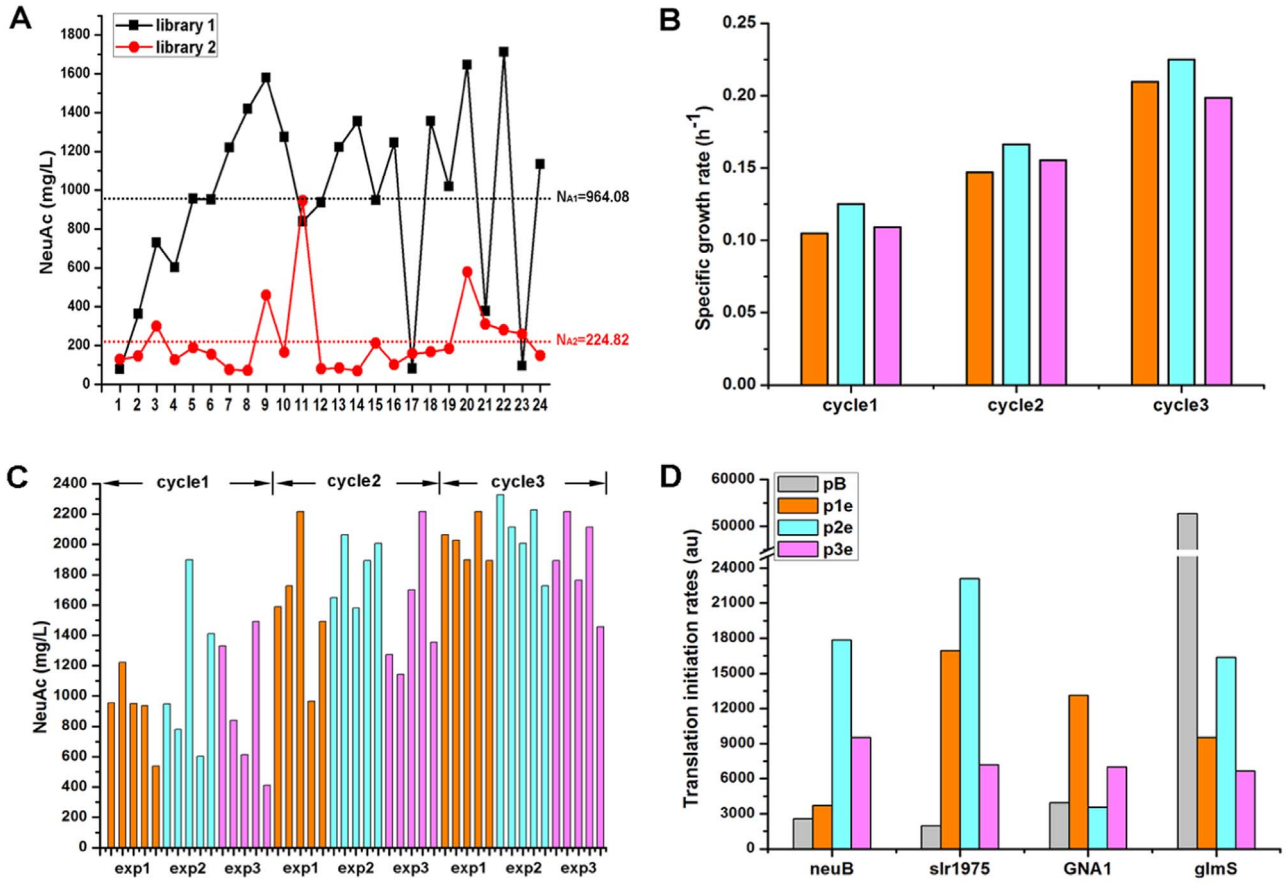

Fig. 5. RBSs randomization to improve NeuAc production. (A) Fermentation of mutants from the constructed RBS libraries. 24 single colonies from library 1 or library 2 were randomly selected and subjected to fermentation in 24-well microplates. Strains were cultivated in MTB medium for 36 h with 30 g/L glucose. N_{A1} and N_{A2} indicate average NeuAc titer of the mutants from library 1 and library 2, respectively. (B) Specific growth rate of the non-clonal cultures during the three evolution cycles. Three independent experiments were performed: experiment 1 in orange (exp1), experiment 2 in cyan (exp2) and experiment 3 in magenta (exp3). (C) Batch-fermentation of NeuAc for pB variants randomly selected from the three experiments described in Fig. 5B. Strains were cultivated in MTB medium for 36 h with 30 g/L glucose in 24-well microplates. (D) Predicted translation initiation rates for related genes in pB and the enriched plasmids. p1e, p2e and p3e were derived from exp1, exp2 and exp3 respectively. Translation initiation rates of the RBSs were predicted with the RBS Calculator v2.0 (Salis et al., 2009).

Table 2
Batch-fermentation for NeuAc production in engineered *E. coli* strains.[a]

Strains	Enrichment percentage[b]	Biomass (g CDW/L)	Glc consumed (g/L)	NeuAc (g/L)	ManNAc (g/L)	GlcNAc (g/L)	pyruvate (g/L)
DN5/pB	*	6.29 ± 0.12	27.45 ± 0.84	1.58 ± 0.11	1.17 ± 0.16	6.13 ± 0.23	5.01 ± 0.14
DN5/p1e	56.5%	5.91 ± 0.06	26.63 ± 0.42	1.98 ± 0.11	0.82 ± 0.03	2.92 ± 0.32	3.52 ± 0.21
DN5/p2e	45%	6.04 ± 0.01	25.81 ± 0.66	2.12 ± 0.08	0.94 ± 0.23	3.43 ± 0.22	4.40 ± 0.34
DN5/p3e	40.7%	6.42 ± 0.11	26.24 ± 0.22	1.86 ± 0.05	1.07 ± 0.15	4.21 ± 0.18	3.58 ± 0.07

[a] Strains were cultivated in MTB medium for 36 h with 30 g/L glucose in shake flasks. Data shown are the average and standard deviation of three replicates.
[b] The enrichment percentage was determined by the sum of one kind of plasmid dividing total sequenced clones. * indicates evolution experiment was not performed.

Table 3
Characterization of NeuB mutants.

NeuB mutants[a]	Enrichment percentage[b]	NeuAc titer (g/L)[c]	Specific activity (U/mg)[d]
wild type	*	2.01 ± 0.16	28.11 ± 0.77
B1 (T74C)	56.5%	2.24 ± 0.03	30.76 ± 1.12
B2 (C914T, G1018A)	13%	1.68 ± 0.13	27.47 ± 0.58
B3 (A506G, G420A)	45%	2.61 ± 0.04	35.71 ± 0.87
B4 (G283A)	20%	1.93 ± 0.06	28.96 ± 0.81
C1 (C914T)	*	1.42 ± 0.03	17.93 ± 0.52
C2 (G1018A)	*	1.88 ± 0.02	26.5 ± 0.88
C3 (T74C, A506G)	*	2.13 ± 0.21	32.48 ± 0.57

[a] For NeuB evolution, two independent experiments were performed. Mutants B1 and B2 were enriched in experiment group 1. B3 and B4 were enriched in experiment group 2. C1, C2 and C3 were artificially constructed.

[b] The enrichment percentage was determined by the sum of one kind of plasmid dividing total sequenced clones.* indicates evolution experiment was not performed.

[c] NeuB mutants were cloned into p2e (replacing the wild type NeuB) and transformed into DN5 to determine the NeuAc production capacities. Strains were cultivated in MTB medium for 36 h with 30 g/L glucose.

[d] NeuB mutants were cloned into pET28a containing the T7 promoter to determine the enzymatic activities. Target enzymes were purified by Ni-NTA Agarose column, and Purities of enzymes were estimated to be > 90% by Coomassie Blue G-250 stained SDS-PAGE (Supplementary Figure 5).

3.3. Screening random RBS library using the NeuAc biosensor for pathway optimization

Fine-tuning of a specific pathway *via* promoter/RBS engineering is an efficient strategy to balance metabolic flux and thus enhance product titer (Coussement et al., 2014; Zhao et al., 2013). With the designed NeuAc biosensor, we were encouraged to optimize the expression of *glmS*, *GNA1*, *slr1975* and *neuB via* RBS engineering. The same strong RBS (AAGGAGATATACC) was initially used for all genes. Mutant library was generated by randomizing RBSs of the four genes using degenerate primers, followed by Gibson assembly.

We designed two sets of degenerate RBSs here, as shown in Table 1. For library 1, a 24 or 36-variant degenerate RBS sequence was designed for each of the four genes, generating a possible library of 497,664 mutants. For library 2, the same degenerate RBS sequence previously used to optimize a synthetic Entner-Doudoroff pathway (Ng et al., 2015) was adopted for the four genes, generating a possible library of 65,536 mutants. After Gibson assembly, we got ~ 2×10^5 Amp^R CFU per mL recovery culture with positive rates more than 95%. We evaluated the two libraries by performing batch fermentation of randomly selected single colonies. Overall, mutants from library 1 tend to accumulate more NeuAc than those from library 2 with an average titer of 964.1 mg/L (N = 24) and 224.8 mg/L (N = 24), respectively (Fig. 5A). This discrepancy may be due to the low expression of related genes for mutants in library 2 (Supplementary Table 3). Library 1 was then used for further study.

To perform genetic selection, the *tetA*-NeuAc biosensor was cloned into a p15Aori plasmid that is compatible with pB, generating p15A-S (Nakano et al., 1995). Mutant library was then transformed into DN5 harboring p15A-S and a three-cycle evolution process was performed as stated above. After each cycle, plasmids were extracted and re-transformed into fresh parental strain to prevent the adaptation of cells to nickel.

For each cycle, cultures were subjected to single colony isolation and ~ 30 randomly selected colonies were sequenced. Specific growth rate of the non-clonal cultures for each cycle was also determined. The growth of non-clonal cultures became better along with the evolution, and the specific growth rate reached ~ 0.2 after cycle 3 (Fig. 5B). Then, single colonies were randomly selected and analyzed with respect to their NeuAc accumulation. As shown in Fig. 5C, strains from cycle 3 produced more NeuAc than those from cycle 1 or cycle 2, indicating the increased growth rate of the non-clonal cultures was due to the enrichment of high NeuAc producers.

Three plasmids p1e, p2e and p3e were enriched to a ratio more than 40% after cycle3 (Table 2, Supplementary Figure 4, Supplementary Table 4). We then evaluated the enriched strains. As a result, all the three strains produced more NeuAc than the original strain DN5/pB. DN5/p2e produced 2.12 ± 0.08 g/L NeuAc (~ 34% improved compared with DN5/pB), the highest among tested strains. Glucose consumption rates and biomass accumulation of the three strains were comparable to that of DN5/pB, but the concentration of intermediates GlcNAc, ManNAc and pyruvate decreased (Table 2). We estimated translation initiation rates of the RBSs in the plasmids. As shown in Fig. 5D, predicted RBS strengths of *neuB*, *slr1975* and *GNA1* were higher in p1e, p2e and p3e than those in pB, except for *GNA1* in p2e, but the strength of *glmS* was less. A too strong expression of *glmS* may increase the accumulation of the upstream intermediate GlcN-6-P while increase of *slr1975* and *neuB* expression may accelerate the conversion of intermediates to NeuAc. This speculation was supported by the decrease of GlcNAc and ManNAc accumulation in the enriched strains (Table 2).

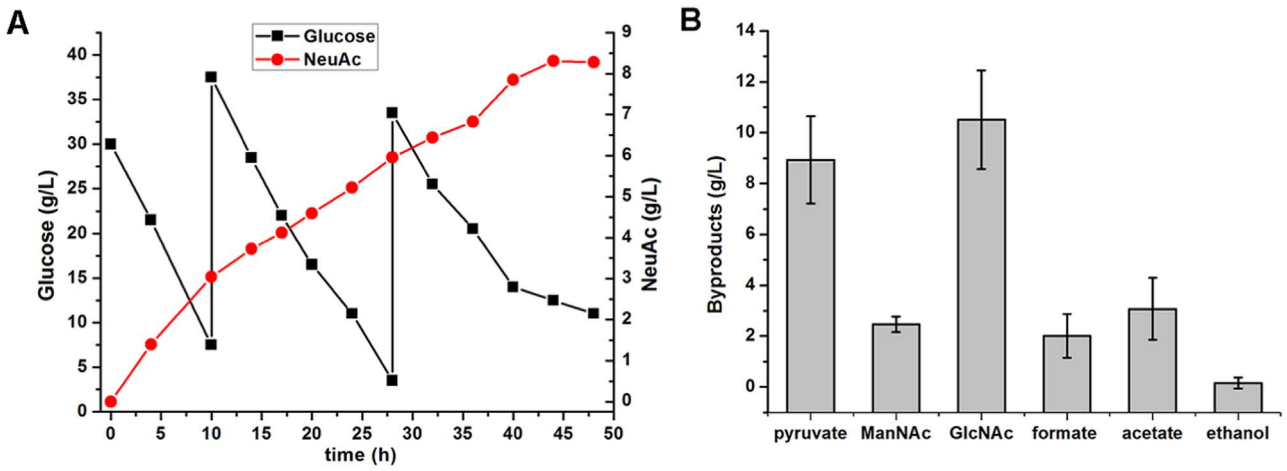

Fig. 6. Fermentation profile of DN5/pB3 for NeuAc production. (A) NeuAc accumulation and glucose consumption during fermentation. Fermentation was performed in a 300-mL baffled shake flask containing 50 mL solution buffer (44 mM KH_2PO_4, 137 mM K_2HPO_4 and 75 mM $(NH_4)_2SO_4$) at 37 °C and 180 rpm, and pH was maintained at approximate 7.0. For clarification, a representative curve from three independent experiments was shown, with standard differences (RSD) less than 10%. (B) Byproducts formation in the supernatants of samples at 44 h.

3.4. Evolution of NeuAc synthase using the NeuAc biosensor

Accumulation of pyruvate, GlcNAc and ManNAc (Table 2) indicates a bottleneck in GlcNAc epimerization or NeuAc synthesis. We thus chose the NeuAc synthase (NeuB) to increase its *in vivo* activity using biosensor-facilitated mutagenesis. To differentiate enzymatic activities of various NeuB mutants easily and ensure that intracellular NeuAc concentration would lie in the response range of the biosensor, a low copy vector (pCL1920, 3–5 copies/cell) was used. The NeuAc pathway genes together with RBSs from p2e were cloned into pCL1920, generating plasmid p4ks. The mutagenetic *neuB* gene generated by error-prone PCR was used to replace the wild type *neuB* on p4ks.

The evolution process was stopped after four cycles and at least 20 randomly selected colonies were sequenced (Table 3). Variants B1 and B3 reached to 56.5% and 45% of the total population, respectively. Two other mutants, B2 and B4 were also enriched, although to a lesser extent. The four most enriched NeuB mutants were cloned into p2e (replacing the wild type NeuB) to evaluate the NeuAc production capacities. Both B1 and B3 produced more NeuAc than the wild type NeuB. DN5/pB1 produced 2.24 ± 0.03 g/L NeuAc, while DN5/pB3 produced 2.61 ± 0.04 g/L (23% improved than DN5/p2e). Specific activity of B3 was 27% improved than the wild type and B1 was also slightly higher than the wild type (9.4% improved).

To test the effect of single amino acid change and combinational sites mutation on enzymatic activity and NeuAc titer, NeuB mutants C1, C2 and C3 were constructed. Unfortunately, these efforts did not improve the NeuAc titer further. NeuAc condensation was considered to be the rate-limiting step for NeuAc production. By increasing the expression of the reversible NanA, a nine-fold increase in NeuAc titer was observed (Lin et al., 2013). Our results here confirmed the importance of the last step in NeuAc biosynthesis, improved enzyme activity of which would provide a strong pull and enhance the carbon flux to NeuAc production.

To evaluate the NeuAc production potential of DN5/pB3, we performed two-stage fermentation in minimal medium. After initial growth stage, cells were transferred to production medium. As shown in Fig. 6A, DN5/pB3 produced 8.31 g/L NeuAc after 44 h. Only small quantity of ManNAc, formate, acetate and ethanol were detected, but considerable amounts of pyruvate and GlcNAc accumulated (Fig. 6B). Pyruvate accumulation may suggest an insufficient of dissolved oxygen (thus a shortage of ATP supply) and this can be remitted using bioreactor fermentation. GlcNAc accumulation was due to the catalytic characteristic of Slr1975. This reversible enzyme uses ATP as activator and is inhibited by excess pyruvate. It has a relatively low affinity for ATP, which limited the catalytic efficiency (Zhang et al., 2010). So GlcNAc 2-epimerases with other sources can be attempted (Klermund et al., 2013; Lee et al., 2007; Sola-Carvajal et al., 2012). Additionally, modification of the host strain to accelerate glutamine regeneration and increase PEP supply may also be beneficial.

4. Conclusion

Biosensor has played a key role to associate genotype to phenotype in large-scale screening of mutant strains. Here, we engineered an *in vivo* active NeuAc responsive biosensor and applied it for growth-coupled selection of high NeuAc producer. Through RBS optimization and NeuB evolution, we obtained a mutant with 8.31 g/L NeuAc production from glucose in minimal medium, establishing a valuable platform for further optimization. The NeuAc biosensor provides a widely applicable tool for discovering and engineering enzymes in the NeuAc pathway and may be suggestive for development of other aptazyme-based biosensors.

Competing interests

The authors declare that they have no competing interests.

Acknowledgements

This study was financially supported by grants from the National Natural Science Foundation of China (31670077) and State Key Laboratory of Microbial Technology.

Appendix A. Supporting information

Supplementary data associated with this article can be found in the online version at http://dx.doi.org/10.1016/j.ymben.2017.08.001.

References

Alper, H., Moxley, J., Nevoigt, E., Fink, G.R., Stephanopoulos, G., 2006. Engineering yeast transcription machinery for improved ethanol tolerance and production. Science 314, 1565–1568.
Bassalo, M.C., Liu, R., Gill, R.T., 2016. Directed evolution and synthetic biology applications to microbial systems. Curr. Opin. Biotechnol. 39, 126–133.
Binder, S., Schendzielorz, G., Stabler, N., Krumbach, K., Hoffmann, K., Bott, M., Eggeling, L., 2012. A high-throughput approach to identify genomic variants of bacterial metabolite producers at the single-cell level. Genome Biol. 13, R40.
Bradford, M.M., 1976. A rapid and sensitive method for the quantitation of microgram quantities of protein utilizing the principle of protein-dye binding. Anal. Biochem. 72, 248–254.
Ceres, P., Garst, A.D., Marcano-Velazquez, J.G., Batey, R.T., 2013. Modularity of select riboswitch expression platforms enables facile engineering of novel genetic regulatory devices. ACS Synth. Biol. 2, 463–472.
Cho, S., Lee, B.R., Cho, B.K., Kim, J.H., Kim, B.G., 2013. *In vitro* selection of sialic acid specific RNA aptamer and its application to the rapid sensing of sialic acid modified sugars. Biotechnol. Bioeng. 110, 905–913.
Coussement, P., Maertens, J., Beauprez, J., Van Bellegem, W., De Mey, M., 2014. One step DNA assembly for combinatorial metabolic engineering. Metab. Eng. 23, 70–77.
DeLoache, W.C., Russ, Z.N., Narcross, L., Gonzales, A.M., Martin, V.J., Dueber, J.E., 2015. An enzyme-coupled biosensor enables (*S*)-reticuline production in yeast from glucose. Nat. Chem. Biol. 11, 465–471.
Deng, M.D., Severson, D.K., Grund, A.D., Wassink, S.L., Burlingame, R.P., Berry, A., Running, J.A., Kunesh, C.A., Song, L., Jerrell, T.A., Rosson, R.A., 2005. Metabolic engineering of *Escherichia coli* for industrial production of glucosamine and *N*-acetylglucosamine. Metab. Eng. 7, 201–214.
Desai, S.K., Gallivan, J.P., 2004. Genetic screens and selections for small molecules based on a synthetic riboswitch that activates protein translation. J. Am. Chem. Soc. 126, 13247–13254.
Gibson, D.G., Young, L., Chuang, R.Y., Venter, J.C., Smith, H.O., 2009. Enzymatic assembly of DNA molecules up to several hundred kilobases. Nat. Methods 6, 343.
Hooks, D.O., Blatchford, P.A., Rehm, B.H., 2013. Bioengineering of bacterial polymer inclusions catalyzing the synthesis of *N*-acetylneuraminic acid. Appl. Environ. Microbiol. 79, 3116–3121.
Ji, W., Sun, W., Feng, J., Song, T., Zhang, D., Ouyang, P., Gu, Z., Xie, J., 2015. Characterization of a novel *N*-acetylneuraminic acid lyase favoring *N*-acetylneuraminic acid synthesis. Sci. Rep. 5, 9341.
Joyce, G.F., 2004. Directed evolution of nucleic acid enzymes. Annu. Rev. Biochem. 73, 791–836.
Kang, J., Gu, P., Wang, Y., Li, Y., Yang, F., Wang, Q., Qi, Q., 2012. Engineering of an *N*-acetylneuraminic acid synthetic pathway in *Escherichia coli*. Metab. Eng. 14, 623–629.
Klermund, L., Groher, A., Castiglione, K., 2013. New *N*-acyl-D-glucosamine 2-epimerases from cyanobacteria with high activity in the absence of ATP and low inhibition by pyruvate. J. Biotechnol. 168, 256–263.
Lee, Y.C., Wu, H.M., Chang, Y.N., Wang, W.C., Hsu, W.H., 2007. The central cavity from the (alpha/alpha)6 barrel structure of *Anabaena* sp. CH1 *N*-acetyl-D-glucosamine 2-epimerase contains two key histidine residues for reversible conversion. J. Mol. Biol. 367, 895–908.
Li, Y., Li, M., Zhang, X., Yang, P., Liang, Q., Qi, Q., 2013. A novel whole-phase succinate fermentation strategy with high volumetric productivity in engineered *Escherichia coli*. Bioresour. Technol. 149, 333–340.
Liang, Q., Qi, Q., 2014. From a co-production design to an integrated single-cell biorefinery. Biotechnol. Adv. 32, 1328–1335.
Lin, B.X., Zhang, Z.J., Liu, W.F., Dong, Z.Y., Tao, Y., 2013. Enhanced production of *N*-acetyl-D-neuraminic acid by multi-approach whole-cell biocatalyst. Appl. Microbiol. Biotechnol. 97, 4775–4784.
Liu, D., Evans, T., Zhang, F., 2015. Applications and advances of metabolite biosensors for metabolic engineering. Metab. Eng. 31, 35–43.
Lynch, S.A., Desai, S.K., Sajja, H.K., Gallivan, J.P., 2007. A high-throughput screen for synthetic riboswitches reveals mechanistic insights into their function. Chem. Biol. 14, 173–184.
Michener, J.K., Smolke, C.D., 2012. High-throughput enzyme evolution in *Saccharomyces cerevisiae* using a synthetic RNA switch. Metab. Eng. 14, 306–316.
Michener, J.K., Thodey, K., Liang, J.C., Smolke, C.D., 2012. Applications of genetically-encoded biosensors for the construction and control of biosynthetic pathways. Metab. Eng. 14, 212–222.
Muranaka, N., Sharma, V., Nomura, Y., Yokobayashi, Y., 2009. An efficient platform for genetic selection and screening of gene switches in *Escherichia coli*. Nucleic Acids Res.

37, e39.
Nakano, Y., Yoshida, Y., Yamashita, Y., Koga, T., 1995. Construction of a series of pACYC-derived plasmid vectors. Gene 162, 157–158.
Ng, C.Y., Farasat, I., Maranas, C.D., Salis, H.M., 2015. Rational design of a synthetic Entner-Doudoroff pathway for improved and controllable NADPH regeneration. Metab. Eng. 29, 86–96.
Raman, S., Rogers, J.K., Taylor, N.D., Church, G.M., 2014. Evolution-guided optimization of biosynthetic pathways. Proc. Natl. Acad. Sci. USA 111, 17803–17808.
Rogers, J.K., Taylor, N.D., Church, G.M., 2016. Biosensor-based engineering of biosynthetic pathways. Curr. Opin. Biotechnol. 42, 84–91.
Salis, H.M., Mirsky, E.A., Voigt, C.A., 2009. Automated design of synthetic ribosome binding sites to control protein expression. Nat. Biotechnol. 27, 946–950.
Sola-Carvajal, A., Sanchez-Carron, G., Garcia-Garcia, M.I., Garcia-Carmona, F., Sanchez-Ferrer, A., 2012. Properties of BoAGE2, a second *N*-acetyl-D-glucosamine 2-epimerase from *Bacteroides ovatus* ATCC 8483. Biochimie 94, 222–230.
Tang, S.Y., Qian, S., Akinterinwa, O., Frei, C.S., Gredell, J.A., Cirino, P.C., 2013. Screening for enhanced triacetic acid lactone production by recombinant *Escherichia coli* expressing a designed triacetic acid lactone reporter. J. Am. Chem. Soc. 135, 10099–10103.
Tao, F., Zhang, Y., Ma, C., Xu, P., 2010. Biotechnological production and applications of *N*-acetyl-D-neuraminic acid: current state and perspectives. Appl. Microbiol. Biotechnol. 87, 1281–1289.
Uchida, Y., Tsukada, Y., Sugimori, T., 1984. Purification and properties of *N*-acetylneuraminate lyase from *Escherichia coli*. J. Biochem. 96, 507–522.
Wang, H.H., Isaacs, F.J., Carr, P.A., Sun, Z.Z., Xu, G., Forest, C.R., Church, G.M., 2009. Programming cells by multiplex genome engineering and accelerated evolution. Nature 460, 894–898.
Wang, J., Gao, D., Yu, X., Li, W., Qi, Q., 2015. Evolution of a chimeric aspartate kinase for L-lysine production using a synthetic RNA device. Appl. Microbiol. Biotechnol. 99, 8527–8536.
Warnecke, T.E., Lynch, M.D., Karimpour-Fard, A., Sandoval, N., Gill, R.T., 2008. A genomics approach to improve the analysis and design of strain selections. Metab. Eng. 10, 154–165.
Watstein, D.M., McNerney, M.P., Styczynski, M.P., 2015. Precise metabolic engineering of carotenoid biosynthesis in *Escherichia coli* towards a low-cost biosensor. Metab. Eng. 31, 171–180.
Win, M.N., Smolke, C.D., 2007. A modular and extensible RNA-based gene-regulatory platform for engineering cellular function. Proc. Natl. Acad. Sci. USA 104, 14283–14288.
Winkler, W.C., Nahvi, A., Roth, A., Collins, J.A., Breaker, R.R., 2004. Control of gene expression by a natural metabolite-responsive ribozyme. Nature 428, 281–286.
Xu, P., Li, L., Zhang, F., Stephanopoulos, G., Koffas, M., 2014. Improving fatty acids production by engineering dynamic pathway regulation and metabolic control. Proc. Natl. Acad. Sci. USA 111, 11299–11304.
Zhang, F., Carothers, J.M., Keasling, J.D., 2012. Design of a dynamic sensor-regulator system for production of chemicals and fuels derived from fatty acids. Nat. Biotechnol. 30, 354–359.
Zhang, M.M., Wang, Y., Ang, E.L., Zhao, H., 2016. Engineering microbial hosts for production of bacterial natural products. Nat. Prod. Rep. 33, 963–987.
Zhang, Y., Tao, F., Du, M., Ma, C., Qiu, J., Gu, L., He, X., Xu, P., 2010. An efficient method for *N*-acetyl-D-neuraminic acid production using coupled bacterial cells with a safe temperature-induced system. Appl. Microbiol. Biotechnol. 86, 481–489.
Zhao, J., Li, Q., Sun, T., Zhu, X., Xu, H., Tang, J., Zhang, X., Ma, Y., 2013. Engineering central metabolic modules of *Escherichia coli* for improving beta-carotene production. Metab. Eng. 17, 42–50.
Zhou, L.B., Zeng, A.P., 2015. Engineering a lysine-ON riboswitch for metabolic control of lysine production in *Corynebacterium glutamicum*. ACS Synth. Biol. 4, 1335–1340.